



1 **Real-time measurements of gas-phase organic acids using SF₆⁻ chemical ionization**
2 **mass spectrometry**

3
4 Theodora Nah,¹ Yi Ji,^{1,2} David J. Tanner,¹ Hongyu Guo,¹ Amy P. Sullivan,³ Nga Lee Ng,^{1,2}
5 Rodney J. Weber¹ and L. Gregory Huey^{1*}

6
7 ¹*School of Earth and Atmospheric Sciences, Georgia Institute of Technology, Atlanta, GA, USA*

8 ²*School of Chemical and Biomolecular Engineering, Georgia Institute of Technology, Atlanta, GA, USA*

9 ³*Department of Atmospheric Science, Colorado State University, Fort Collins, CO, USA*

10

11 * *To whom correspondence should be addressed: greg.huey@eas.gatech.edu*

12

13 **Abstract**

14 The sources and atmospheric chemistry of gas-phase organic acids are currently poorly
15 understood due in part to the limited range of measurement techniques available. In this
16 work, we evaluated the use of SF₆⁻ as a sensitive and selective chemical ionization reagent
17 ion for real-time measurements of gas-phase organic acids. Field measurements are made
18 using a chemical ionization mass spectrometer (CIMS) at a rural site in Yorkville, Georgia
19 from September to October 2016 to investigate the capability of this measurement
20 technique. Our measurements demonstrate that SF₆⁻ can be used to measure a range of
21 organic acids in the atmosphere. Ambient concentrations of organic acids ranged from a
22 few parts per trillion by volume (ppt) to several parts per billion by volume (ppb).
23 Assuming that these organic acids are completely water-soluble, the carbon mass fraction
24 of gas-phase water-soluble organic carbon (WSOC_g) comprised of these organic acids
25 ranged from 7 to 100 % with a study average of 30 %. All the organic acids displayed
26 similar strong diurnal behaviors, reaching maximum concentrations between 5 and 7 pm
27 local time. The organic acid concentrations are dependent on ambient temperature, with
28 higher organic acid concentrations being measured during warmer periods.

29 **Introduction**

30 Organic acids are ubiquitous and important species in the troposphere. They are
31 major contributors of free acidity in precipitation (Galloway et al., 1982; Keene et al., 1983;
32 Keene and Galloway, 1984), and can also affect the formation of secondary organic
33 aerosols (SOA) (Zhang et al., 2004; Carlton et al., 2006; Sorooshian et al., 2010; Yatavelli



34 et al., 2015). As end products of oxidation, organic acids can also serve as useful tracers of
35 air mass history (Sorooshian et al., 2007; Sorooshian et al., 2010). Organic acids are found
36 in urban, rural and remote marine environments in the gas, aqueous and particle phases.
37 While organic acids are emitted directly from biogenic sources (e.g., microbial activity,
38 vegetation and soil) and anthropogenic activities (e.g., fossil fuel combustion, vehicular
39 emissions and biomass burning) (Kawamura et al., 1985; Talbot et al., 1988; Chebbi and
40 Carlier, 1996; Talbot et al., 1999; Seco et al., 2007; Veres et al., 2010; Paulot et al., 2011;
41 Veres et al., 2011; Millet et al., 2015), they can also be formed from photooxidation of
42 non-methane volatile organic compounds and aqueous-phase photochemistry of semi-
43 volatile organic compounds (Chebbi and Carlier, 1996; Hansen et al., 2003; Orzechowska
44 and Paulson, 2005; Carlton et al., 2006; Sorooshian et al., 2007; Ervens et al., 2008; Paulot
45 et al., 2011; Millet et al., 2015). The chemical aging of organic aerosols has also been
46 proposed as a major source of organic acids (Paulot et al., 2011). The relative importance
47 of primary and secondary sources of organic acids are currently poorly constrained though
48 their emissions likely depend on the magnitude of biogenic and anthropogenic activities
49 and the meteorological conditions. Wet and dry deposition are the primary sinks of organic
50 acids in the atmosphere (Chebbi and Carlier, 1996).

51 Formic and acetic acids are the dominant gas-phase monocarboxylic acids in the
52 troposphere (Chebbi and Carlier, 1996). Due to their high vapor pressures, the gas-phase
53 concentrations of formic and acetic acids are usually 1 to 2 orders of magnitudes higher
54 than their particle-phase concentrations. Some field studies report strong correlations
55 between formic and acetic acids, suggesting that these two organic acids have similar
56 sources (Nolte et al., 1997; Souza and Carvalho, 2001; Paulot et al., 2011). A recent
57 modeling study suggested that the dominant sources of formic acid in the southeastern U.S.
58 are primarily biogenic in nature (Millet et al., 2015). These sources include direct emissions
59 from vegetation and soil and photochemical production from biogenic volatile organic
60 compounds (BVOCs). Currently, atmospheric formic and acetic acid concentrations are
61 higher than those predicted by models, indicating that present model estimates of source
62 and sink magnitudes are incorrect (Paulot et al., 2011; Millet et al., 2015). In the case of
63 formic acid, deposition and secondary photochemical production via mechanisms such as
64 photooxidation of isoprene and reaction of stabilized criegee intermediates need to be



65 better constrained in models. Given that formic and acetic acids are major trace gases in
66 the atmosphere, there is a need to resolve the discrepancy between measurements and
67 model predictions to close the atmospheric reactive carbon budget and improve our overall
68 understanding of VOC chemistry in the atmosphere.

69 Currently, research on gas-phase organic acids has focused primarily on formic and
70 acetic acids (Andreae et al., 1988; Talbot et al., 1988; Grosjean, 1991; Hartmann et al.,
71 1991; Talbot et al., 1995; Talbot et al., 1999). This is due, in part, to the analytical
72 difficulties in measuring gas-phase $> C_2$ organic acids and oxidized organic acids (i.e.,
73 containing more than 2 oxygen atoms) in real time. These organic acids have low vapor
74 pressures and are generally present in low concentrations in the gas phase. For example,
75 dicarboxylic acids typically have vapor pressures that are 2 to 4 orders of magnitude lower
76 than their analogous monocarboxylic acids (Chebbi and Carlier, 1996), and are present
77 mainly in the particle and aqueous phases. Rapid and accurate measurements of gas-phase
78 $> C_2$ organic acids and oxidized organic acids are necessary for constraining the regional
79 and global SOA budget since these acids can partition readily between the gas and particle
80 and aqueous phases and subsequently affect SOA formation (Zhang et al., 2004; Carlton
81 et al., 2006; Ervens et al., 2008; Sorooshian et al., 2010; Yatavelli et al., 2015).

82 Chemical ionization mass spectrometry (CIMS) is commonly used to selectively
83 measure atmospheric trace gases in real-time with high sensitivity. CIMS measurements
84 rely on reactions between reagent ions and compounds of interest present in the sampled
85 air to produce analyte ions that are detected by a mass spectrometer. The subset of
86 molecular species detected is determined by the reagent ion employed since the specificity
87 of the ionization process is governed by the ion-molecule reaction mechanism. CIMS is a
88 popular tool for atmospheric measurements since it provides high time resolution, linear
89 and reproducible measurements. It is also a soft ionization technique with minimal ion
90 fragmentation, thus preserving the parent molecule's elemental composition and allowing
91 for molecular speciation. Recent developments in chemical ionization methods and sources
92 have greatly improved our ability to measure atmospheric acidic species. Some of the
93 CIMS reagent ions that have been used to measure atmospheric organic acids include
94 acetate ($CH_3CO_2^-$), iodide (I^-) and CF_3O^- anions (Crounse et al., 2006; Veres et al., 2008;



95 Lee et al., 2014; Brophy and Farmer, 2015; Nguyen et al., 2015). However, each of these
96 CIMS reagent ions has its drawbacks, which are generally related to their selectivity and
97 sensitivity towards different atmospheric species. For example, acetic acid is difficult to
98 measure with CH_3CO_2^- as the CIMS reagent ion due to interferences from the reagent ion
99 chemistry that complicates the desired ion-molecule reactions. In addition, while many
100 organic acids can be detected using I^- as a reagent ion, its sensitivity to different acids can
101 vary by orders of magnitude (Lee et al., 2014). For these reasons, this work is focused on
102 assessing the ability of SF_6^- to measure a series of organic acids in ambient air.

103 The sulfur hexafluoride (SF_6^-) anion has been used as a CIMS reagent ion to
104 measure atmospheric inorganic species such as sulfur dioxide (SO_2), nitric acid (HNO_3)
105 and peroxyxynitric acid (HO_2NO_2) (Slusher et al., 2001; Slusher et al., 2002; Huey et al.,
106 2004; Kim et al., 2007). SF_6^- commonly reacts with most acidic gases at the collision rate
107 by either proton or fluoride transfer reactions (Huey et al., 1995). However, SF_6^- is reactive
108 to both ozone (O_3) and water vapor, which can lead to interfering reactions that limit its
109 applicability to many species in certain environments (Huey et al., 2004). In this work, we
110 present ambient measurements of gas-phase organic acids conducted in a mixed forest-
111 agricultural area in Georgia in early fall of 2016 to evaluate the performance of a SF_6^-
112 CIMS technique. Gas-phase organic acid measurements are compared to gas-phase water-
113 soluble organic carbon (WSOC_g) measurements performed during the field study to
114 estimate the fraction of WSOC_g that is comprised of organic acids at this rural site.
115 Laboratory experiments are conducted to measure the sensitivity of SF_6^- with a series of
116 organic acids of atmospheric relevance.

117 2. Methods

118 2.1. Field site

119 Real-time ambient measurements of gas-phase organic acids were obtained using a
120 chemical ionization mass spectrometer from 3 Sept to 12 Oct 2016 at the SouthEastern
121 Aerosol Research and Characterization (SEARCH) site located in Yorkville, Georgia. A
122 detailed description of the field site has been provided by Hansen et al. (2003). Briefly, the
123 Yorkville field site (33.931 N, 85.046 W) was located ~55 km northwest of Atlanta, and



124 was on a broad ridge in a large pasture where there were occasionally grazing cattle. The
125 field site was surrounded by forest and agricultural land. There were no major roads near
126 the field site and nearby traffic emissions were negligible. The sampling period was
127 characterized by moderate temperatures (24.0 °C average, 32.6 °C max, 9.5 °C min) and
128 high relative humidities (68.9% RH average, 100% RH max, 21.6% RH min). The study-
129 averaged diurnal trends of relative humidity, temperature and solar radiance are shown in
130 Fig. S1. Data reported are displayed in EDT. Volumetric gas concentrations reported are
131 at ambient temperature and relative humidity.

132 2.2. SF₆ CIMS

133 2.2.1. CIMS instrument and air sampling inlet

134 The CIMS instrument was housed in a temperature controlled trailer during the
135 field study. The inlet configuration and CIMS instrument used in this study is shown in
136 Fig. 1. Since HNO₃ and organic acids may condense on surfaces, an inlet configuration
137 with a minimal wall interaction was used. This inlet configuration was previously described
138 by Huey et al. (2004) and Nowak et al. (2006); hence, only a brief description will be
139 provided here. The inlet was a 7.6 cm ID aluminum pipe that extended ~40 cm into the
140 ambient air through a hole in the trailer's wall. This positioned the inlet ~2 m above the
141 ground. A donut-shaped ring was attached to the ambient sampling port of the pipe to
142 reduce the influence of crosswinds on the pipe's flow dynamics. This ring was wrapped
143 with a fine wire mesh to prevent insects from being drawn through the pipe. A flow of
144 ~2800 L min⁻¹ was maintained in the pipe using a regenerative blower (AMETEK
145 Windjammer 116637-03). Part of this flow (7 L min⁻¹) was sampled through a custom-
146 made three-way PFA Teflon valve, which connected the pipe's center to the CIMS
147 sampling orifice. The valve was maintained at a temperature of 40 °C in an insulated
148 aluminum oven and could be switched automatically between ambient and background
149 modes. In ambient mode, ambient air was passed through a 25 cm long, 0.65 cm ID Teflon
150 tube into the CIMS. In background mode, ambient air was first drawn through an activated
151 charcoal scrubber before being delivered into the CIMS. A small flow of ambient air
152 (~0.05 L min⁻¹) was continuously passed through the scrubber to keep it at equilibrium
153 with ambient humidity levels. Most of the sampled air flow (6.7 L min⁻¹) was exhausted



154 using a small diaphragm pump. The rest of the sampled air flow (0.3 L min^{-1}) was
155 introduced into the CIMS instrument through an automatic variable orifice, which was used
156 to maintain a constant sample air mass flow.

157 Detailed descriptions of the CIMS instrument can be found in Liao et al. (2011) and
158 Chen et al. (2016). Briefly, the CIMS instrument was comprised of a series of differentially
159 pumped regions: a flow tube, a collisional dissociation chamber, an octopole ion guide, a
160 quadrupole mass filter and an ion detector. These sections were evacuated by a scroll pump
161 (Varian TriscrollTM 300), a drag pump (Adixen MDP 5011) and two turbo pumps (Varian
162 Turbo-V70), respectively. Ambient air was drawn continuously into the flow tube. A flow
163 of 3.7 L min^{-1} of N_2 containing a few ppm of SF_6 (Scott-Marrin Inc.) was passed through
164 a ^{210}Po ion source into the flow tube. SF_6^- anions, which were produced via associative
165 electron attachment in the ^{210}Po ion source, reacted with the sampled ambient air in the
166 flow tube to generate analyte ions. The flow tube was maintained at a low pressure (~ 13
167 mbar) to minimize interferences from SF_6^- reaction with water vapor. The analyte ions then
168 exited the flow tube and were accelerated through the collisional dissociation chamber
169 (CDC), which was maintained at ~ 0.8 mbar. The molecular collisions in the CDC served
170 to dissociate weakly bound cluster ions into their core ions to simplify mass spectral
171 analysis. For this study, the CDC was operated at a relatively high voltage (-50 V) to
172 efficiently dissociate cluster ions. The resulting ions were then passed into the octopole ion
173 guide (maintained at $\sim 6 \times 10^{-3}$ mbar), which collimated the ions and transferred them into
174 the quadrupole mass spectrometer (maintained at $\sim 10^{-5}$ mbar) for mass selection and
175 detection.

176 **2.2.2. Background and calibration measurements during field study**

177 Background measurements were performed every 25 min during the field study.
178 During each background measurement, the sampled air flow was passed through an
179 activated charcoal scrubber prior to delivery into the CIMS. The scrubber removed $> 99 \%$
180 of the targeted species in ambient air. Calibration measurements were performed every 5 h
181 during the field study through standard additions of $^{34}\text{SO}_2$ and either formic or acetic acid
182 to the sampled air flow. Each background and calibration measurement period lasted ~ 4
183 min. A $1.12 \text{ ppm } ^{34}\text{SO}_2$ gas standard was used as the source of the sulfur standard addition.



184 The formic and acetic acid calibration sources were permeation tubes (VICI Metronics)
185 with emission rates of 91 and 110 ng min⁻¹, respectively. The emission rates were measured
186 by scrubbing the output of the permeation tube in deionized water via a gas impinge
187 immersed in water, which was then analyzed for formate and acetate using ion
188 chromatography (Thermo Fisher Scientific). Eight samples of each acid were analyzed
189 over the course of the field study and the standard deviations of the permeation rates were
190 ≤ 6 %. The CIMS instrument sensitivity measured by the F₂³⁴SO₂⁻ ion signal (m/z 104) was
191 similarly applied to all the other measured species (except for formic and acetic acids)
192 using relative sensitivities determined in laboratory studies. The F₂³⁴SO₂⁻ calibrant ion
193 signals were also used to calibrate ambient F₂³²SO₂⁻ ion signals and determine ambient SO₂
194 concentrations as discussed in section 3.2.5.

195 2.2.3. Laboratory calibration

196 HNO₃, oxalic, butyric, glycolic, propionic and valeric acid standard addition
197 calibrations were performed in post-field laboratory work. The response of the CIMS acid
198 signals were measured relative to the sensitivity of ³⁴SO₂ in these calibration
199 measurements. The HNO₃ calibration source was a permeation tube (KIN-TEK) with a
200 permeation rate of 39 ng min⁻¹, which was measured using UV optical absorption (Neuman
201 et al., 2003). Solid or liquid samples of oxalic (Sigma Aldrich, ≥ 99 %), butyric (Sigma
202 Aldrich, ≥ 99 %), glycolic (Sigma Aldrich, 99 %), propionic (Sigma Aldrich, ≥ 99.5 %)
203 and valeric (Sigma Aldrich, ≥ 99 %) acids were used in calibration measurements. The acid
204 sample was placed in a glass impinger, which was immersed in an ice bath to provide a
205 constant vapor pressure. A flow of 6 to 10 mL min⁻¹ of N₂ was passed over the organic acid
206 in the glass impinger. This organic acid air stream was then diluted with varying flows of
207 N₂ (1 to 5 L min⁻¹) to achieve different mixing ratios of the organic acid. Mixing ratios
208 were calculated from either the acid's emission rate from the impinger or the acid's vapor
209 pressure. The emission rate of gas-phase oxalic acid from the impinger was measured by
210 scrubbing the output in deionized water using the same method for calibrating the formic
211 and acetic acid permeation tubes, followed by ion chromatography analysis for oxalate.
212 Three samples were analyzed and the emission rate was determined to be 14 ng min⁻¹ with
213 a standard deviation of < 5 %. The vapor pressures of butyric and propionic acids at 0 °C



214 were measured using a capacitance manometer (MKS Instruments). The vapor pressures
215 of glycolic and valeric acids at 0 °C were estimated using their literature vapor pressures
216 at 25 °C and enthalpies of vaporization (Daubert and Danner, 1989; Lide, 1995; Acree and
217 Chickos, 2010).

218 Attempts to generate a calibration plot for pyruvic acid using its liquid sample
219 (Sigma Aldrich, 98 %) and the setup described above were unsuccessful as this acid was
220 found to interact very strongly with surfaces. Glyoxylic acid calibrations were not
221 performed due to the presence of impurities in the glyoxylic acid monohydrate solution
222 used (Sigma Aldrich, 98 %), which resulted in the appearance of ions not attributed to
223 glyoxylic acid. We attempted to generate calibration plots for malonic (Sigma Aldrich, ≥
224 99.5 %), succinic (Sigma Aldrich, 99 %) and glutaric (Sigma Aldrich, 99 %) acids by
225 passing N₂ over their solid samples at room temperature. However, it was not possible to
226 generate large enough gas phase concentrations for calibration since these organic acids
227 have very low vapor pressures.

228 **2.2.4. Detection limits and measurement uncertainties**

229 The detection limits of the organic acids were approximated from 3 times the
230 standard deviation values (3σ) of the ion signals measured during background mode. Table
231 1 summarizes the average detection limits of the organic acids for 2.5 min integration
232 periods which corresponds to the length of a background measurement with a 0.04 s duty
233 cycle for each m/z. The mean difference between successive background measurements
234 ranged from 1 to 40 ppt for the different organic acids. Future work will focus on reducing
235 the instrument background, and therefore improving the detection limits of these organic
236 acids.

237 The uncertainties (1σ) in our ambient measurements of formic, acetic and oxalic
238 acid concentrations originated from CIMS and IC calibration measurements. The IC
239 measurement uncertainty was estimated to be 10 %. For formic and acetic acids, which
240 were calibrated during the field study using permeation tubes, their CIMS measurement
241 uncertainties were estimated to be 6 and 7 %, respectively, based on one standard deviation
242 of the acids' calibrant ion signals. For oxalic acid which was calibrated in post-field



243 laboratory work, the CIMS measurement uncertainty was estimated to be 9 % based on one
244 standard deviation of the $^{34}\text{SO}_2$ sensitivity (3 %), the acid's calibrant ion signals (7 %) and
245 linear fit of the calibration curve (5 %). Hence, the uncertainties in our ambient
246 measurements of formic, acetic and oxalic acid concentrations were estimated to be 12, 12
247 and 14 %, respectively.

248 For nitric acid which was calibrated in post-field laboratory work using a
249 permeation tube and UV optical absorption, the uncertainty in its ambient concentrations
250 was estimated to be 9 % based on uncertainties in UV absorption measurements (3 %) and
251 one standard deviation of the $^{34}\text{SO}_2$ sensitivity (3 %) and acid's calibrant ion signals (8 %).
252 For butyric and propionic acids which were calibrated in post-field laboratory work using
253 vapor pressures measured by a capacitance manometer, the uncertainties in their ambient
254 concentrations were estimated to be 14 % based on the vapor pressure measurement
255 uncertainty (10 %) and one standard deviation of the $^{34}\text{SO}_2$ sensitivity (3 %), the acids'
256 calibrant ion signals (8 %) and linear fits of the acids' calibration curves (3 %). For glycolic
257 and valeric acids which were calibrated in post-field laboratory work using vapor pressures
258 estimated from literature vapor pressures at 25 °C and enthalpies of vaporization, the
259 uncertainties in their ambient concentrations were likely significantly larger compared to
260 the other measured organic acids due to uncertainties in their estimated vapor pressures.
261 We estimate the uncertainties in ambient concentrations of glycolic and valeric acids to be
262 22 % based on an assumed vapor pressure uncertainty of 20 % and one standard deviation
263 of the $^{34}\text{SO}_2$ sensitivity (3 %), the acids' calibrant ion signals (8 %) and linear fits of the
264 acids' calibration curves (2 %).

265 **2.3. WSOC_g measurements**

266 WSOC_g was measured with a MIST chamber coupled to a total organic carbon
267 (TOC) analyzer (Sievers 900 series, GE Analytical Instruments). Ambient air first passed
268 through a Teflon filter (45 mm diameter, 2.0 μm pore size, Pall Life Sciences) to remove
269 particles in the air stream. This filter was changed every 3 to 4 days. The particle-free air
270 was then pulled into a glass Mist Chamber filled with ultrapure deionized water at a flow
271 rate of 20 L min⁻¹. The MIST chamber scrubbed soluble gases with Henry's law constants
272 greater than 10³ M atm⁻¹ into deionized water (Spaulding et al., 2002). The resulting liquid



273 samples from the MIST chamber were analyzed by the TOC analyzer. The TOC analyzer
274 converted the organic carbon in the liquid samples to carbon dioxide using UV light and
275 chemical oxidation. The carbon dioxide formed was then measured by conductivity. The
276 amount of organic carbon in the liquid samples is proportional to the measured increase in
277 conductivity of the dissolved carbon dioxide. Each WSOC_g measurement lasted 4 min.
278 Background WSOC_g measurements were performed for 45 min every 12 h by stopping the
279 sample air flow and rinsing the sampling lines with deionized water. The TOC analyzer
280 was calibrated using different concentrations of sucrose (as specified by the instrument
281 manual) before and after the field study. The limit of detection was 0.4 μgC m⁻³. The
282 measurement uncertainty was estimated to be 10 % based on uncertainties in the sample
283 air flow, liquid flow and TOC analyzer uncertainty. The MIST chamber and upstream
284 particle filter were located in an air-conditioned building so were generally below ambient
285 temperature. Hence, evaporation of collected particles (which will lead to positive artifacts
286 in WSOC_g measurements) are not expected to be significant.

287 **2.4. Supporting gas measurements**

288 Supporting gas measurements were provided by a suite of instruments operated by
289 the SEARCH network. A non-dispersive infrared spectrometer (Thermo Fisher Scientific)
290 provided hourly CO measurements. A UV absorption analyzer (Thermo Fisher Scientific)
291 provided hourly O₃ measurements. A gas chromatography-flame ionization detector (GC-
292 FID, Agilent Technologies) provided hourly VOC measurements.

293 **3. Results and discussion**

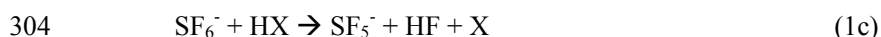
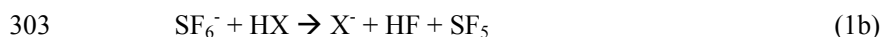
294 **3.1. General SF₆⁻ CIMS field performance**

295 **3.1.1. SF₆⁻ ion chemistry with organic acids**

296 The underlying aspect of CIMS measurements of atmospheric constituents is the
297 use of ion-molecule reactions to selectively ionize compounds of interest in the complex
298 matrix of ambient air and produce characteristic ions. The reactions of SF₆⁻ with the organic
299 acids (HX) gave similar products to those reported previously for SF₆⁻ reactions with

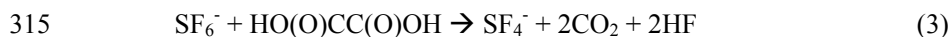
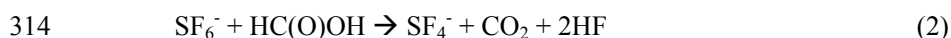


300 inorganic acids (Huey et al., 1995): SF_5^- , X^- and $\text{X}^-\cdot\text{HF}$ where X^- is the conjugate base of
301 the organic acid (reactions 1a-c).



305 The SF_5^- ion (m/z 127, reaction 1c) is a common reaction product of the reactions of SF_6^-
306 with many species and is probably thermodynamically driven by the formation of HF
307 (Huey et al., 1995). Unfortunately, the production of SF_5^- does not allow for the selective
308 detection of any atmospheric species. In addition, the larger the branching ratio of the SF_5^-
309 channel, the lower the CIMS sensitivity to an individual acid since the effective rate
310 constants for the X^- and $\text{X}^-\cdot\text{HF}$ channels are lower.

311 The reaction of SF_6^- with formic acid and oxalic acid also produced SF_4^- ions (m/z
312 108). These reactions are probably thermodynamically driven by the formation of CO_2 and
313 HF:



316 We used the X^- and/or $\text{X}^-\cdot\text{HF}$ ions to determine ambient organic acid concentrations
317 since these ions are characteristic of the individual acids. For all the organic acids, the X^-
318 $\cdot\text{HF}$ ion signal is substantially lower than that of the X^- ion for the conditions in this study.
319 However, this is probably largely due to the relatively high collision energy used in the
320 CDC which led to efficient dissociation of the fluoride adducts to form X^- ions.
321 Consequently, only the proton transfer channel (1b) is used to quantify most of the organic
322 acids in the field study. The exceptions are formic and acetic acid as discussed in section
323 3.2.1 and 3.2.2 Table 1 shows a summary of the sensitivities of X^- and $\text{X}^-\cdot\text{HF}$ ions of
324 organic acids relative to that of the $\text{F}_2^{34}\text{SO}_2^-$ ion.

325 3.1.2. Characterization of interferences



326 SF_6^- is very sensitive to many trace atmospheric species but its reactions with water
327 vapor and O_3 when sampling ambient air can lead to issues both with selectivity and
328 stability. For example, SF_6^- reacts nonlinearly with water vapor to form a series of $\text{F}^-\cdot(\text{HF})_n$
329 cluster ions (Huey et al., 1995; Arnold and Viggiano, 2001). SF_6^- also reacts efficiently
330 with O_3 to form O_3^- , which is rapidly converted to CO_3^- in ambient air (Slusher et al., 2001).
331 These reactions can deplete SF_6^- as well as form a variety of potentially interfering ions
332 that depend on more abundant atmospheric species. For these reasons, efforts were made
333 to minimize interferences by limiting reaction times and the flow sampled into the CIMS.
334 This was accomplished by sampling only 0.3 L min^{-1} of air through the variable orifice into
335 the flow tube which was maintained at a pressure of ~ 13 mbar. Figure 2 shows a mass
336 spectrum of ambient air. Interference peaks at m/z 39 ($\text{F}^-\cdot(\text{HF})$ and CO_3^- , respectively) can
337 be attributed to the presence of water and O_3 , respectively. Figure S2a shows the time series
338 of the $^{34}\text{SF}_6^-$ reagent ion signal and ambient water vapor concentration for the entire field
339 study. Despite fluctuations in ambient water vapor concentrations, the $^{34}\text{SF}_6^-$ reagent ion
340 signal was relatively constant for the entire field study with a standard deviation of $< 3\%$.
341 This indicates that the reaction of SF_6^- with ambient water vapor (and O_3) did not
342 significantly deplete the SF_6^- reagent ions during the field study.

343 The $\text{F}_2^{34}\text{SO}_2^-$ ion signal was used to monitor the CIMS SO_2 sensitivity during the
344 field study. Figure S2b shows the time series of the $\text{F}_2^{34}\text{SO}_2^-/^{34}\text{SF}_6^-$ ion signal ratio obtained
345 in calibration measurements. There is a noticeable increase in the $\text{F}_2^{34}\text{SO}_2^-/^{34}\text{SF}_6^-$ ion signal
346 ratio on 28 Sept 2016, indicating an increase in the CIMS instrument sensitivity. The
347 increase in CIMS instrument sensitivity is due to the decrease in ambient water vapor
348 concentrations on 28 Sept 2016 (Fig. S2a). Previous laboratory and field studies showed
349 that this was due to the hydrolysis of $\text{F}_2^{34}\text{SO}_2^-$, which led to the loss of this ion and
350 diminished sensitivity at higher levels of ambient water vapor (Arnold and Viggiano, 2001;
351 Slusher et al., 2001). However, the SO_2 sensitivity at $\text{F}_2^{34}\text{SO}_2^-$ only varied within a factor
352 of two for the entire field study with a clear relationship to water vapor (Fig. S2c). The X^-
353 and $\text{X}^-\cdot\text{HF}$ ions of formic and acetic acids do not show any obvious dependence on ambient
354 water vapor concentration during calibration measurements. Therefore, we do not expect
355 the sensitivities of the X^- and $\text{X}^-\cdot\text{HF}$ ions of the studied organic acids to depend on ambient
356 water vapor concentrations. We accounted for water vapor dependence of the $\text{F}_2^{34}\text{SO}_2^-$ ion



357 signal in our post-field calibrations where the response of the CIMS acid signals were
358 measured relative to the of the $^{34}\text{SO}_2$ sensitivity.

359 **3.2. Ambient measurements**

360 **3.2.1. Formic acid**

361 Figure 2 shows typical mass spectra obtained under background and measurement
362 modes during the field study. The SF_6^- reagent ion is present at m/z 146. One of the
363 prominent species in the mass spectrum is formic acid, which is detected as HCOO^- and
364 $\text{HCOO}^- \cdot \text{HF}$ at m/z 45 and 65, respectively. Our laboratory studies demonstrated that the
365 reaction of formic acid with SF_6^- also produced a large fraction of SF_4^- ions at m/z 108.
366 The reaction of SF_6^- with oxalic acid also produced SF_4^- ions, but its SF_4^- product ion yield
367 is low and gas phase oxalic acid is not present in large concentrations. In addition, SF_4^- is
368 present in the mass spectrum obtained under background mode but the SF_4^- background
369 ion signals are lower than those typically observed in measurement mode at the Yorkville
370 site. As a result, we determined the ambient formic acid concentrations using the HCOO^- ,
371 $\text{HCOO}^- \cdot \text{HF}$ and SF_4^- ions. Figure 3a shows a scatter plot comparing the ambient formic
372 acid concentrations measured at Yorkville using the HCOO^- , $\text{HCOO}^- \cdot \text{HF}$ and SF_4^- ions.
373 Linear regression analysis reveals that the formic acid concentrations determined by the
374 three ions are highly correlated ($R^2 = 0.99$) with slopes exhibiting a near 1:1 correlation.
375 The excellent correlation between these three ions and the agreement with laboratory data
376 indicates that formic acid is selectively measured by this method.

377 The time series of formic acid, temperature and solar radiation measured at
378 Yorkville are shown in Fig. 3b. Formic acid concentrations ranged from 0.04 to 4 ppb
379 during the field study, with strong and consistent diurnal trends. The day-to-day variability
380 in formic acid concentrations are associated with changes in solar radiation and
381 temperature. Higher formic acid concentrations are measured during warm and sunny days,
382 similar to formic acid measurements performed in Centreville, rural Alabama during the
383 2013 Southern Oxidant Aerosol Study (SOAS) (Brophy and Farmer, 2015; Millet et al.,
384 2015). Figure 3c shows the study-averaged diurnal profiles of formic acid and solar
385 irradiance. Formic acid started to increase at 7:30, which coincided with a sharp increase



386 in solar irradiance. Concentrations continued to increase throughout the day and peaked at
387 18:30, which coincided with the approximate time just before solar irradiance reached zero.
388 Formic acid then decreased continuously throughout the night.

389 The immediate early-morning increase in formic acid observed in this field study
390 is similar to that seen during the SOAS study (Millet et al., 2015). However, there are some
391 differences in the formic acid diurnal cycles measured in this field study and the SOAS
392 study. Formic acid peaked at 15:30 during SOAS, approximately 3 hours before solar
393 irradiance decreased to zero. In contrast, formic acid concentrations only started to
394 decrease at sunset (at 19:30) in this study. This suggests that there may be differences in
395 the types and/or magnitudes of formic acid sources and sinks in this two field studies. Land
396 cover and/or land use differences may have contributed to differences in formic acid
397 sources and sinks at the Centreville and Yorkville field sites. The area surrounding the
398 Yorkville field site is covered primarily by hardwood mixed with farmland and open
399 pastures. In contrast, the Centreville field site is surrounded by forests comprised of mixed
400 oak-hickory and loblolly trees (Hansen et al., 2003). It is also possible that seasonal
401 differences contributed to differences in formic acid sources and sinks in the two field
402 studies. The SOAS campaign took place in the middle of summer (1 June to 15 July 2013)
403 when biogenic emissions are typically higher while this field study took place in early fall
404 when biogenic emissions are lower due to cooler temperatures. For example, the average
405 concentration of isoprene (a formic acid source) in this study (1.21 ppb) is lower than that
406 in SOAS (1.92 ppb (Millet et al., 2015)). Despite these differences, our overall results are
407 similar to the formic acid measurements performed in SOAS in both magnitude and diurnal
408 variability.

409 3.2.2. Acetic acid

410 Acetic acid is detected with SF_6^- as CH_3COO^- and $\text{CH}_3\text{COO}^- \cdot \text{HF}$ at m/z 59 and 79,
411 respectively. However, these ions are subject to interferences from the reaction of SF_6^- with
412 water vapor present in the sampled ambient air. Two of these interfering ions $\text{F}^- \cdot (\text{HF})_2$ and
413 $\text{F}^- \cdot (\text{HF})_3$ occur at m/z 59 and 79, respectively. As discussed earlier, we minimized the
414 impact of these interferences by diluting the sample flow into the CIMS and running the
415 CDC at a high collision energy to dissociate the HF cluster ions. As expected from cluster



416 bond strengths, we found that larger HF cluster ions dissociated more easily than smaller
417 ones. For example, at a CDC electric field of $\sim 113 \text{ V cm}^{-1}$ (the configuration used in this
418 field study), virtually all of the $\text{F}^{\bullet}(\text{HF})_3$ cluster ions dissociated while very few of the F^{\bullet}
419 (HF) cluster ions dissociated. This indicates that the m/z 79 channel for acetic acid is more
420 immune to interference from water vapor than the m/z 59 channel. This is supported by the
421 observation that the background ion signal at m/z 59 ($R^2 = 0.50$) is more highly correlated
422 with ambient water vapor concentrations than the background ion signal of m/z 79 ($R^2 =$
423 0.30). In addition, the m/z 59 ion is subjected to interference from the reaction of SF_6^- with
424 O_3 present in the sampled ambient air. SF_6^- reacts with O_3 in the presence of CO_2 to form
425 CO_3^- at m/z 60 (Slusher et al., 2001). As shown in Fig. 2, the large CO_3^- peak at m/z 60 is
426 a potential interference to the m/z 59 signal. As the background scrubber also removed O_3
427 from the ambient air, there is a large difference in the m/z 60 ion signal between the
428 measurement and background modes ($\sim 100,000 \text{ Hz}$). Thus, even a few percent bleed over
429 of m/z 60 to m/z 59 can lead to an over-estimation of ambient acetic acid concentrations.
430 For these reasons, we used m/z 79 ($\text{X}^{\bullet}\text{HF}$) to determine ambient acetic acid concentrations
431 even though this channel has a lower sensitivity than the m/z 59 channel (X^-).

432 The time series of acetic acid, temperature and solar radiation measured at
433 Yorkville are shown in Fig. 4a. Acetic acid concentrations ranged from 0.03 to 3 ppb during
434 the field study. The day-to-day variability in acetic acid concentrations resembled the
435 behavior of formic acid concentrations, with higher concentrations being measured during
436 warm and sunny days. Figure 4b shows the study-averaged diurnal profiles of acetic acid
437 and solar irradiance. The diurnal profile of acetic acid is similar to that of formic acid with
438 a more pronounced evening maximum. Acetic acid started to increase at 7:30 and built up
439 through the day, peaking at 19:30 and decreased continuously overnight. In general, acetic
440 acid concentrations are well correlated with ($R^2 = 0.67$) and comparable in magnitude (~ 60
441 % on average) to formic acid. The study-averaged formic acid/acetic acid concentration
442 ratio (1.65) is comparable to ratios from previous field studies in rural and urban
443 environments (Talbot et al., 1988; Talbot et al., 1995; Granby et al., 1997; Khare et al.,
444 1999; Talbot et al., 1999; Baboukas et al., 2000; Singh et al., 2000; Kuhn et al., 2002;
445 Baasandorj et al., 2015; Millet et al., 2015).



446 3.2.3. Larger organic acids

447 In addition to formic acid and acetic acid, eight other ions were monitored during
448 the field study: m/z 73, 75, 87, 89, 101, 103, 117 and 131. These ions were chosen as they
449 had significant signals when ambient air was sampled and were not obviously formed from
450 SF_6^- reaction with water vapor or O_3 . Since the CIMS utilized in this study only had unit
451 mass resolution, these ions are the sum of all organic acid isomers and isobaric organic
452 acids of the same molecular weight as well as other product ions from species that might
453 react with SF_6^- . However, real-time ion chromatography measurements of aerosol
454 composition performed during the field study demonstrated the presence of particulate
455 oxalic, malonic, succinic and glutaric acids (Nah et al., 2018). For this reason, for m/z 89,
456 103, 117 and 131 ions, we assigned them as X^- ions of oxalic, malonic, succinic and glutaric
457 acids, respectively. As these organic acids have low vapor pressures, their gas-phase
458 concentrations are expected to be lower than their particle-phase concentrations, though
459 their gas-particle ratios will depend on thermodynamic conditions (Nah et al., 2018).
460 Particulate formic acid and acetic acid were also detected by ion chromatography during
461 the field study, but were at much lower concentrations relative to the gas phase (Nah et al.,
462 2018). For simplicity, we also denoted m/z 73, 75, 87 and 101 ions as X^- ions of propionic,
463 glycolic, butyric and valeric acids, respectively, for the remainder of this paper. These
464 organic acids have previously been measured in rural and urban environments (Kawamura
465 et al., 1985; Veres et al., 2011; Brophy and Farmer, 2015). However, we note that these
466 assignments are speculative. Post-field calibration measurements were used to estimate the
467 ambient concentrations of these organic acids.

468 Figure 5 shows the time series and diurnal profiles of oxalic, butyric, glycolic,
469 propionic and valeric acids measured during the field study. Daytime concentrations of
470 these organic acids ranged from a few tens of ppt to several hundred ppt. The time series
471 of ion signals of malonic, succinic and glutaric acids are shown in Fig. S3. Concentrations
472 of these organic acids are not available since calibrations were not performed for these
473 compounds. The eight organic acids displayed very similar day-to-day variability as formic
474 and acetic acids, with higher concentrations (or ion signals) being measured on warm and
475 sunny days. The diurnal profiles of all the measured organic acids have similar diurnal



476 trends, with their concentrations reaching a maximum between 17:30 and 19:30 and rapidly
477 decreasing after sunset.

478 **3.2.4. Comparison with WSOC_g**

479 WSOC_g measurements were performed during the field study using a MIST
480 chamber coupled to a TOC analyzer. The study average WSOC_g was $3.6 \pm 2.7 \mu\text{gC m}^{-3}$,
481 slightly lower than that measured during the SOAS study ($4.9 \mu\text{gC m}^{-3}$) (Xu et al., 2017),
482 and approximately four times lower than that measured in urban Atlanta, Georgia (13.7
483 $\mu\text{gC m}^{-3}$) (Hennigan et al., 2009). Despite being comparable in magnitude, the diurnal
484 profiles of WSOC_g measured in this study and the SOAS study are different. WSOC_g
485 measured in the SOAS study decreased at sunset, while WSOC_g measured in this study
486 decreased 2 hours after sunset. Differences in WSOC_g concentrations and diurnal profiles
487 at the three different sites may be due to differences in emission sources as a result of
488 different measurement periods, land use and/or land cover.

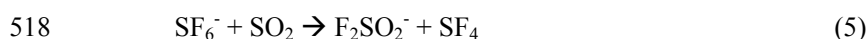
489 To estimate the fraction of WSOC_g that is comprised of organic acids, the total
490 organic carbon contributed by formic, acetic, oxalic, butyric, glycolic, propionic and
491 valeric acids is compared to the WSOC_g measurements. Figures 6a and 6b show the time
492 series and diurnal profiles of WSOC_g and the organic carbon contributed by the measured
493 organic acids. Formic and acetic acids comprised majority of the total organic carbon
494 contributed by the measured organic acids (study averages of 31 and 38 %, respectively).
495 Assuming that the measured organic acids are completely water-soluble, the carbon mass
496 fraction of WSOC_g comprised of these organic acids ranged from 7 to 100 %. Based on the
497 orthogonal distance regression slope shown in Fig. 6c, the study-averaged carbon mass
498 fraction of WSOC_g comprised of the measured organic acids is 30 %. The total organic
499 carbon contributed by the measured organic acids are moderately correlated with WSOC_g
500 ($R^2 = 0.38$). This is likely due to the presence of other water-soluble gas phase species
501 (with different day-to-day variability from the organic acids) that contribute to the WSOC_g.
502 This is supported by slight differences in the diurnal profiles of WSOC_g and the organic
503 carbon contributed by the organic acids (Fig. 6b). While the diurnal profiles of WSOC_g
504 and the organic carbon contributed by the organic acids have similar general shapes,
505 WSOC_g peaked at 21:30, approximately 2 hours after the solar irradiance have decreased



506 to zero. In contrast, the organic carbon contributed by the organic acids start to decrease at
507 sunset (at 19:30).

508 3.2.5. SO₂ and HNO₃ observations

509 In addition to evaluating the field performance of the SF₆⁻ CIMS technique in gas-
510 phase organic acid measurements, another focus of this study was to investigate the
511 possible sources of the measured organic acids. For this reason, HNO₃ and SO₂ (two
512 common anthropogenic tracers) were also measured by SF₆⁻ CIMS during the field study.
513 Correlations between the concentrations of organic acids and those of HNO₃ and SO₂ were
514 then examined to determine if the organic acids were anthropogenic in nature (section 3.3).
515 While their reactions with SF₆⁻ have multiple product channels (Huey et al., 1995), only
516 the NO₃⁻•HF (m/z 82) and F₂SO₂⁻ (m/z 102) ions were used for quantitative purposes:



519 Figure S4 shows the time series of SO₂ and HNO₃ measured during the field study.
520 As expected at a rural site, SO₂ and HNO₃ concentrations are low most of the time (study
521 averages of 0.23 and 0.18 ppb, respectively). However, there were occasional periods when
522 the site was impacted by anthropogenic pollution. In particular, there are spikes in both
523 SO₂ and HNO₃ concentrations throughout the study that corresponded to the site being
524 impacted by power plant or urban emissions. Outside of these anthropogenic spikes, HNO₃
525 showed a clear diurnal profile with a maximum at approximately 12:30, consistent with
526 local photochemical production.

527 3.3. Potential sources of organic acids

528 Correlation analysis on organic acid concentrations can provide insights on their
529 sources. Figure 7 shows that the concentration of formic acid is strongly correlated with
530 those of the other measured organic acids ($R^2 = 0.68$ to 0.89). This suggests that these
531 organic acids have the same or similar sources at Yorkville. The sources of organic acids
532 can be biogenic or anthropogenic in nature. To determine if the primary sources of organic
533 acids are of biogenic or anthropogenic origin, we first examined the correlations of organic



534 acid concentrations with those of anthropogenic pollutants CO, SO₂, O₃ and HNO₃. CO
535 and SO₂ are common tracers for combustion sources. The organic acid concentrations are
536 poorly correlated with CO (Fig. S5, R² = 0.03 to 0.15) and SO₂ (Fig. S6, R² = 0.01 to 0.24),
537 indicating that primary emissions from combustion are a minor source of organic acids in
538 Yorkville. HNO₃ and O₃ are common photochemical tracers of urban air masses. The
539 organic acid concentrations are weakly correlated with O₃ (Fig. S7, R² = 0.11 to 0.32) and
540 HNO₃ (Fig. S8, R² = 0.33 to 0.56). In addition, there is no noticeable increase in organic
541 acid concentrations during periods of elevated CO, SO₂, O₃ and HNO₃ concentrations when
542 the site was impacted by pollution plumes. Together, these results indicate that the primary
543 sources of organic acids in Yorkville are likely not anthropogenic in nature.

544 Diurnal profiles of the measured organic acids suggest that their sources are linked
545 to higher daytime temperatures and/or photochemical processes. Figure 8 compares the
546 concentrations of organic acids against ambient temperatures measured during the study.
547 Since there was a noticeable decrease in mean ambient temperatures starting on 28 Sept
548 2016, we grouped the datasets into two time periods (3 to 27 Sept and 28 Sept to 12 Oct)
549 to better evaluate the effect of temperature on organic acid concentrations. The average
550 temperature in the first time period (3 to 27 Sept) is 24.8 °C (32.6 °C max, 18.1 °C min),
551 while the average temperature in the second time period (28 Sept to 12 Oct) is 19.5 °C
552 (28.4 °C max, 9.5 °C min). We find that organic acid concentrations are on average higher
553 and more highly correlated with temperatures in the warmer first time period (R² = 0.40 to
554 0.63) compared to the cooler second time period (R² = 0.18 to 0.59). These observations
555 can be explained by temperature-dependent emissions of organic acids and their BVOC
556 precursors. Previous studies have shown that emissions of organic acids and their BVOC
557 precursors depend strongly on light and temperature, with substantially lower
558 concentrations being emitted in the dark and/or at low temperatures (Kesselmeier et al.,
559 1997; Kesselmeier, 2001; Sindelarova et al., 2014). We find that the concentration of
560 isoprene, which was the dominant BVOC in Yorkville, has a somewhat similar diurnal
561 profile as the organic acids and decreased with temperature on 28 Sept 2016 (Fig. S9). In
562 addition, the concentrations of formic and acetic acids are moderately correlated with that
563 of isoprene (R² = 0.42 and 0.40, respectively) (Fig. S10).



564 Multiphase photochemical aging of ambient organic aerosols can also be a source
565 of gas-phase organic acids (Eliason et al., 2003; Ervens et al., 2004; Molina et al., 2004;
566 Lim et al., 2005; Park et al., 2006; Walser et al., 2007; Sorooshian et al., 2007; Vlasenko
567 et al., 2008; Pan et al., 2009; Sorooshian et al., 2010). Organic acids may be formed in the
568 particle phase during organic aerosol photochemical aging, with subsequent volatilization
569 into the gas phase. Real-time ion chromatography measurements of aerosol composition
570 demonstrated the presence of particulate formic, acetic, oxalic, malonic, succinic and
571 glutaric acids (Nah et al., 2018). However, since the ratios of gas-phase formic and acetic
572 acid mass concentration to the total organic aerosol mass concentration are large (study
573 averages of 40 and 35 %, respectively) (Nah et al., 2018), it is unlikely that organic aerosol
574 photochemical aging is a large source of formic and acetic acids. In contrast, the ratios of
575 gas-phase oxalic, malonic, succinic and glutaric acids mass concentration to the total
576 organic aerosol mass concentration are small, suggesting that organic aerosol
577 photochemical aging may be an important source of these gas-phase organic acids.

578 In summary, the temperature dependence and diurnal profile of organic acid
579 concentrations combined with poor correlations between organic acid concentrations and
580 those of anthropogenic pollutants CO, SO₂, O₃ and HNO₃ strongly suggest that the primary
581 sources of gas-phase organic acids at Yorkville are biogenic in nature. However, our data
582 alone does not allow us to determine if the organic acids are a result of direct emissions or
583 photochemical oxidation of other BVOC emissions and/or organic aerosols. Partitioning
584 of these organic acids between the gas and particle phases will be discussed in a
585 forthcoming paper (Nah et al., 2018).

586 **4. Summary**

587 SF₆⁻ reacted with all of the studied organic acids to produce product ions that were
588 characteristic of the individual acids (i.e., X⁻ or X⁻•HF). These reactions all occurred at less
589 than the maximum collisional rate due to significant yields of SF₅⁻ and SF₄⁻, which reduced
590 the sensitivity of the method. For the conditions employed in this study, the sensitivities of
591 X⁻ and X⁻•HF ions of the organic acids relative to that of the F₂³⁴SO₂⁻ ion (study-averaged
592 sensitivity 2928 ± 669 Hz ppb⁻¹) ranged from 0.04 to 2.18. The detection limits of the
593 organic acids were approximated from 3 times the standard deviation values (3σ) of the ion



594 signals obtained during background measurements. Reasonable limits of detection for 2.5
595 min integration periods (1 to 60 ppt) were obtained for all the organic acids studied. Water
596 vapor and O₃ can lead to interferences with this method but for the conditions employed in
597 this study, they were largely limited to acetic acid measurements at m/z 59. However,
598 fluctuations in ambient water vapor can also lead to changes in sensitivity for the detection
599 of some species (e.g., SO₂). Uncertainties in organic acid concentrations originate primarily
600 from calibration measurements and ranged from 9 to 22 %. Overall, the tractable mass
601 spectra obtained by the SF₆⁻ CIMS method coupled with reasonable limits of detection and
602 the high correlations observed between the individual organic acids demonstrated the
603 potential of this method. Obvious next steps for the SF₆⁻ CIMS method are to compare it
604 to other measurement methods for organic acids and to deploy the SF₆⁻ ion chemistry to a
605 higher resolution time-of-flight mass spectrometer to reduce the potential for interferences.

606 The SF₆⁻ CIMS method was deployed for measurements of gas phase organic acids
607 in a mixed forest-agricultural area in Yorkville, Georgia from Sept to Oct 2016. The
608 organic acids measured in the field study were formic and acetic acids. In addition,
609 measurements tentatively assigned to oxalic, butyric, glycolic, propionic, valeric, malonic,
610 succinic and glutaric acids were performed. Ambient concentrations of these organic acids
611 ranged from a few ppt to several ppb. All the organic acids exhibited similar strong diurnal
612 trends. Organic acid concentrations built up throughout the day, peaked between 17:30 and
613 19:30 before decreasing continuously overnight. Strong correlations between organic acid
614 concentrations indicated that these organic acids likely have the same or similar sources at
615 Yorkville. We concluded that the organic acids were likely not due to anthropogenic
616 emissions since they were poorly correlated with anthropogenic pollutants and their
617 concentrations were not elevated when the site was impacted by pollution plumes. Higher
618 organic acid concentrations were measured during warm and sunny days. Organic acid
619 concentrations were strongly correlated with temperature during the first month of the
620 study when ambient temperatures were high. Together, our results suggested that the
621 primary sources of organic acids at Yorkville were biogenic in nature. Direct biogenic
622 emissions of organic acids and/or their BVOC precursors were likely enhanced at high
623 ambient temperatures, resulting in the observed variability of organic acid concentrations.
624 Another potential source is the production of organic acids in the particle phase from the



625 multiphase photochemical aging of organic aerosols followed by evaporation to the gas
626 phase, though this source is likely not a large source of formic and acetic acids. However,
627 given the inability of current models and photochemical mechanisms to explain formic acid
628 observations in the Southeastern U.S. (Millet et al., 2015), it is unlikely that our
629 observations of formic acid and larger organic acids can be explained as well. Further work
630 (i.e., laboratory, field and modeling studies) is needed to determine how organic acids are
631 formed in the atmosphere.

632 **5. Acknowledgements**

633 The authors thank Eric Edgerton (Atmospheric Research and Analysis, Inc.) for
634 providing CO, O₃ and VOC measurements and meteorological data.

635 **6. Funding**

636 This publication was developed under US Environmental Protection Agency (EPA)
637 STAR Grant R835882 awarded to Georgia Institute of Technology. It has not been
638 formally reviewed by the EPA. The views expressed in this document are solely those of
639 the authors and do not necessarily reflect those of the EPA. EPA does not endorse any
640 products or commercial services mentioned in this publication.

641 **7. Competing financial interests**

642 The authors declare no competing financial interests.

643 **8. References**

644 Acree, W., and Chickos, J. S.: Phase Transition Enthalpy Measurements of Organic and
645 Organometallic Compounds. Sublimation, Vaporization and Fusion Enthalpies From 1880
646 to 2010, J. Phys. Chem. Ref. Data, 39, 942, 10.1063/1.3309507, 2010.

647 Andreae, M. O., Talbot, R. W., Andreae, T. W., and Harriss, R. C.: Formic and Acetic
648 Acid over the Central Amazon Region, Brazil. 1. Dry Season, Journal of Geophysical
649 Research-Atmospheres, 93, 1616-1624, 10.1029/JD093iD02p01616, 1988.



- 650 Arnold, S. T., and Viggiano, A. A.: Turbulent ion flow tube study of the cluster-mediated
651 reactions of SF₆⁻ with H₂O, CH₃OH, and C₂H₅OH from 50 to 500 torr, *J. Phys. Chem.*
652 *A*, 105, 3527-3531, 10.1021/jp003967y, 2001.
- 653 Baasandorj, M., Millet, D. B., Hu, L., Mitroo, D., and Williams, B. J.: Measuring acetic
654 and formic acid by proton-transfer-reaction mass spectrometry: sensitivity, humidity
655 dependence, and quantifying interferences, *Atmospheric Measurement Techniques*, 8,
656 1303-1321, 10.5194/amt-8-1303-2015, 2015.
- 657 Baboukas, E. D., Kanakidou, M., and Mihalopoulos, N.: Carboxylic acids in gas and
658 particulate phase above the Atlantic Ocean, *Journal of Geophysical Research-*
659 *Atmospheres*, 105, 14459-14471, 10.1029/1999jd900977, 2000.
- 660 Brophy, P., and Farmer, D. K.: A switchable reagent ion high resolution time-of-flight
661 chemical ionization mass spectrometer for real-time measurement of gas phase oxidized
662 species: characterization from the 2013 southern oxidant and aerosol study, *Atmospheric*
663 *Measurement Techniques*, 8, 2945-2959, 10.5194/amt-8-2945-2015, 2015.
- 664 Carlton, A. G., Turpin, B. J., Lim, H. J., Altieri, K. E., and Seitzinger, S.: Link between
665 isoprene and secondary organic aerosol (SOA): Pyruvic acid oxidation yields low volatility
666 organic acids in clouds, *Geophys. Res. Lett.*, 33, 4, 10.1029/2005gl025374, 2006.
- 667 Chebbi, A., and Carlier, P.: Carboxylic acids in the troposphere, occurrence, sources, and
668 sinks: A review, *Atmospheric Environment*, 30, 4233-4249, 10.1016/1352-
669 2310(96)00102-1, 1996.
- 670 Crounse, J. D., McKinney, K. A., Kwan, A. J., and Wennberg, P. O.: Measurement of gas-
671 phase hydroperoxides by chemical ionization mass spectrometry, *Analytical Chemistry*,
672 78, 6726-6732, 10.1021/ac0604235, 2006.
- 673 Daubert, T. E., and Danner, R. P.: Physical and thermodynamic properties of pure
674 chemicals: data compilation, Taylor & Francis, Washington, DC, 1989.



- 675 Eliason, T. L., Aloisio, S., Donaldson, D. J., Cziczo, D. J., and Vaida, V.: Processing of
676 unsaturated organic acid films and aerosols by ozone, *Atmospheric Environment*, 37, 2207-
677 2219, 10.1016/s1352-2310(03)00149-3, 2003.
- 678 Ervens, B., Feingold, G., Frost, G. J., and Kreidenweis, S. M.: A modeling study of aqueous
679 production of dicarboxylic acids: 1. Chemical pathways and speciated organic mass
680 production, *Journal of Geophysical Research-Atmospheres*, 109, 10.1029/2003jd004387,
681 2004.
- 682 Ervens, B., Carlton, A. G., Turpin, B. J., Altieri, K. E., Kreidenweis, S. M., and Feingold,
683 G.: Secondary organic aerosol yields from cloud-processing of isoprene oxidation
684 products, *Geophys. Res. Lett.*, 35, 10.1029/2007gl031828, 2008.
- 685 Galloway, J. N., Likens, G. E., Keene, W. C., and Miller, J. M.: The Composition of
686 Precipitation in Remote Areas of the World, *Journal of Geophysical Research-Oceans and*
687 *Atmospheres*, 87, 8771-8786, 10.1029/JC087iC11p08771, 1982.
- 688 Granby, K., Egelov, A. H., Nielsen, T., and Lohse, C.: Carboxylic acids: Seasonal variation
689 and relation to chemical and meteorological parameters, *Journal of Atmospheric*
690 *Chemistry*, 28, 195-207, 10.1023/a:1005877419395, 1997.
- 691 Grosjean, D.: Ambient Levels of Formaldehyde, Acetaldehyde, and Formic acid in
692 Southern Californic- Results of a One-year Base-line Study, *Environmental Science &*
693 *Technology*, 25, 710-715, 10.1021/es00016a016, 1991.
- 694 Hansen, D. A., Edgerton, E. S., Hartsell, B. E., Jansen, J. J., Kandasamy, N., Hidy, G. M.,
695 and Blanchard, C. L.: The southeastern aerosol research and characterization study: Part 1-
696 overview, *Journal of the Air & Waste Management Association*, 53, 1460-1471, 2003.
- 697 Hartmann, W. R., Santana, M., Hermoso, M., Andreae, M. O., and Sanhueza, E.: Diurnal
698 Cycles of Formic and Acetic Acids in the Northern Part of the Guayana Sheld, Venezuela,
699 *Journal of Atmospheric Chemistry*, 13, 63-72, 10.1007/bf00048100, 1991.



- 700 Hennigan, C. J., Bergin, M. H., Russell, A. G., Nenes, A., and Weber, R. J.: Gas/particle
701 partitioning of water-soluble organic aerosol in Atlanta, *Atmos. Chem. Phys.*, 9, 3613-
702 3628, 10.5194/acp-9-3613-2009, 2009.
- 703 Huey, L. G., Hanson, D. R., and Howard, C. J.: Reactions of SF₆- and I- with Atmospheric
704 Trace Gases, *Journal of Physical Chemistry*, 99, 5001-5008, 10.1021/j100014a021, 1995.
- 705 Huey, L. G., Tanner, D. J., Slusher, D. L., Dibb, J. E., Arimoto, R., Chen, G., Davis, D.,
706 Buhr, M. P., Nowak, J. B., Mauldin, R. L., Eisele, F. L., and Kosciuch, E.: CIMS
707 measurements of HNO₃ and SO₂ at the South Pole during ISCAT 2000, *Atmospheric*
708 *Environment*, 38, 5411-5421, 10.1016/j.atmosenv.2004.04.037, 2004.
- 709 Kawamura, K., Ng, L. L., and Kaplan, I. R.: Determination of Organic Acids (C₁-C₁₀) in
710 the Atmosphere, Motor Exhausts, and Engine Oils, *Environmental Science & Technology*,
711 19, 1082-1086, 10.1021/es00141a010, 1985.
- 712 Keene, W. C., Galloway, J. N., and Holden, J. D.: Measurement of Weak Organic Acidity
713 in Precipitation from Remote Areas of the World, *Journal of Geophysical Research-Oceans*
714 *and Atmospheres*, 88, 5122-5130, 10.1029/JC088iC09p05122, 1983.
- 715 Keene, W. C., and Galloway, J. N.: Organic Acidity in Precipitation of North America,
716 *Atmospheric Environment*, 18, 2491-2497, 10.1016/0004-6981(84)90020-9, 1984.
- 717 Kesselmeier, J., Bode, K., Hofmann, U., Muller, H., Schafer, L., Wolf, A., Ciccioli, P.,
718 Brancaleoni, E., Cecinato, A., Frattoni, M., Foster, P., Ferrari, C., Jacob, V., Fugit, J. L.,
719 Dutaur, L., Simon, V., and Torres, L.: Emission of short chained organic acids, aldehydes
720 and monoterpenes from *Quercus ilex* L. and *Pinus pinea* L. in relation to physiological
721 activities, carbon budget and emission algorithms, *Atmospheric Environment*, 31, 119-133,
722 10.1016/s1352-2310(97)00079-4, 1997.
- 723 Kesselmeier, J.: Exchange of short-chain oxygenated volatile organic compounds (VOCs)
724 between plants and the atmosphere: A compilation of field and laboratory studies, *Journal*
725 *of Atmospheric Chemistry*, 39, 219-233, 10.1023/a:1010632302076, 2001.



- 726 Khare, P., Kumar, N., Kumari, K. M., and Srivastava, S. S.: Atmospheric formic and acetic
727 acids: An overview, *Reviews of Geophysics*, 37, 227-248, 10.1029/1998rg900005, 1999.
- 728 Kim, S., Huey, L. G., Stickel, R. E., Tanner, D. J., Crawford, J. H., Olson, J. R., Chen, G.,
729 Brune, W. H., Ren, X., Leshner, R., Wooldridge, P. J., Bertram, T. H., Perring, A., Cohen,
730 R. C., Lefer, B. L., Shetter, R. E., Avery, M., Diskin, G., and Sokolik, I.: Measurement of
731 HO₂NO₂ in the free troposphere during the intercontinental chemical transport experiment
732 - North America 2004, *Journal of Geophysical Research-Atmospheres*, 112,
733 10.1029/2006jd007676, 2007.
- 734 Kuhn, U., Rottenberger, S., Biesenthal, T., Ammann, C., Wolf, A., Schebeske, G., Oliva,
735 S. T., Tavares, T. M., and Kesselmeier, J.: Exchange of short-chain monocarboxylic acids
736 by vegetation at a remote tropical forest site in Amazonia, *Journal of Geophysical*
737 *Research-Atmospheres*, 107, 18, 10.1029/2000jd000303, 2002.
- 738 Lee, B. H., Lopez-Hilfiker, F. D., Mohr, C., Kurten, T., Worsnop, D. R., and Thornton, J.
739 A.: An Iodide-Adduct High-Resolution Time-of-Flight Chemical-Ionization Mass
740 Spectrometer: Application to Atmospheric Inorganic and Organic Compounds,
741 *Environmental Science & Technology*, 48, 6309-6317, 10.1021/es500362a, 2014.
- 742 Liao, J., Sihler, H., Huey, L. G., Neuman, J. A., Tanner, D. J., Friess, U., Platt, U., Flocke,
743 F. M., Orlando, J. J., Shepson, P. B., Beine, H. J., Weinheimer, A. J., Sjostedt, S. J., Nowak,
744 J. B., Knapp, D. J., Staebler, R. M., Zheng, W., Sander, R., Hall, S. R., and Ullmann, K.:
745 A comparison of Arctic BrO measurements by chemical ionization mass spectrometry and
746 long path-differential optical absorption spectroscopy, *Journal of Geophysical Research-*
747 *Atmospheres*, 116, 10.1029/2010jd014788, 2011.
- 748 Lide, D. R.: *CRC handbook of chemistry and physics: a ready-reference book of chemical*
749 *and physical data*, CRC Press, Boca Raton, FL, 1995.
- 750 Lim, H. J., Carlton, A. G., and Turpin, B. J.: Isoprene forms secondary organic aerosol
751 through cloud processing: Model simulations, *Environmental Science & Technology*, 39,
752 4441-4446, 10.1021/es048039h, 2005.



- 753 Millet, D. B., Baasandorj, M., Farmer, D. K., Thornton, J. A., Baumann, K., Brophy, P.,
754 Chaliyakunnel, S., de Gouw, J. A., Graus, M., Hu, L., Koss, A., Lee, B. H., Lopez-Hilfiker,
755 F. D., Neuman, J. A., Paulot, F., Peischl, J., Pollack, I. B., Ryerson, T. B., Warneke, C.,
756 Williams, B. J., and Xu, J.: A large and ubiquitous source of atmospheric formic acid,
757 *Atmos. Chem. Phys.*, 15, 6283-6304, 10.5194/acp-15-6283-2015, 2015.
- 758 Molina, M. J., Ivanov, A. V., Trakhtenberg, S., and Molina, L. T.: Atmospheric evolution
759 of organic aerosol, *Geophys. Res. Lett.*, 31, 10.1029/2004gl020910, 2004.
- 760 Nah, T., Guo, H., Sullivan, A. P., Chen, Y., Tanner, D. J., Nenes, A., Russell, A., Ng, N.
761 L., Huey, L. G., and Weber, R. J.: Characterization of Aerosol Composition, Aerosol
762 Acidity and Organic Acid Partitioning at an Agriculture-intensive Rural Southeastern U.S.
763 Site, In Preparation, 2018.
- 764 Neuman, J. A., Ryerson, T. B., Huey, L. G., Jakoubek, R., Nowak, J. B., Simons, C., and
765 Fehsenfeld, F. C.: Calibration and evaluation of nitric acid and ammonia permeation tubes
766 by UV optical absorption, *Environmental Science & Technology*, 37, 2975-2981,
767 10.1021/es0264221, 2003.
- 768 Nguyen, T. B., Crouse, J. D., Teng, A. P., Clair, J. M. S., Paulot, F., Wolfe, G. M., and
769 Wennberg, P. O.: Rapid deposition of oxidized biogenic compounds to a temperate forest,
770 *Proc. Natl. Acad. Sci. U. S. A.*, 112, E392-E401, 10.1073/pnas.1418702112, 2015.
- 771 Nolte, C. G., Solomon, P. A., Fall, T., Salmon, L. G., and Cass, G. R.: Seasonal and spatial
772 characteristics of formic and acetic acids concentrations in the southern California
773 atmosphere, *Environmental Science & Technology*, 31, 2547-2553, 10.1021/es960954i,
774 1997.
- 775 Nowak, J. B., Huey, L. G., Russell, A. G., Tian, D., Neuman, J. A., Orsini, D., Sjostedt, S.
776 J., Sullivan, A. P., Tanner, D. J., Weber, R. J., Nenes, A., Edgerton, E., and Fehsenfeld, F.
777 C.: Analysis of urban gas phase ammonia measurements from the 2002 Atlanta Aerosol
778 Nucleation and Real-Time Characterization Experiment (ANARChE), *Journal of*
779 *Geophysical Research-Atmospheres*, 111, 14, 10.1029/2006jd007113, 2006.



- 780 Orzechowska, G. E., and Paulson, S. E.: Photochemical sources of organic acids. 1.
781 Reaction of ozone with isoprene, propene, and 2-butenes under dry and humid conditions
782 using SPME, *J. Phys. Chem. A*, 109, 5358-5365, 10.1021/jp050166s, 2005.
- 783 Pan, X., Underwood, J. S., Xing, J. H., Mang, S. A., and Nizkorodov, S. A.:
784 Photodegradation of secondary organic aerosol generated from limonene oxidation by
785 ozone studied with chemical ionization mass spectrometry, *Atmos. Chem. Phys.*, 9, 3851-
786 3865, 10.5194/acp-9-3851-2009, 2009.
- 787 Park, J., Gomez, A. L., Walser, M. L., Lin, A., and Nizkorodov, S. A.: Ozonolysis and
788 photolysis of alkene-terminated self-assembled monolayers on quartz nanoparticles:
789 implications for photochemical aging of organic aerosol particles, *Physical Chemistry*
790 *Chemical Physics*, 8, 2506-2512, 10.1039/b602704k, 2006.
- 791 Paulot, F., Wunch, D., Crounse, J. D., Toon, G. C., Millet, D. B., DeCarlo, P. F.,
792 Vigouroux, C., Deutscher, N. M., Abad, G. G., Notholt, J., Warneke, T., Hannigan, J. W.,
793 Warneke, C., de Gouw, J. A., Dunlea, E. J., De Maziere, M., Griffith, D. W. T., Bernath,
794 P., Jimenez, J. L., and Wennberg, P. O.: Importance of secondary sources in the
795 atmospheric budgets of formic and acetic acids, *Atmos. Chem. Phys.*, 11, 1989-2013,
796 10.5194/acp-11-1989-2011, 2011.
- 797 Seco, R., Penuelas, J., and Filella, I.: Short-chain oxygenated VOCs: Emission and uptake
798 by plants and atmospheric sources, sinks, and concentrations, *Atmospheric Environment*,
799 41, 2477-2499, 10.1016/j.atmosenv.2006.11.029, 2007.
- 800 Sindelarova, K., Granier, C., Bouarar, I., Guenther, A., Tilmes, S., Stavrakou, T., Muller,
801 J. F., Kuhn, U., Stefani, P., and Knorr, W.: Global data set of biogenic VOC emissions
802 calculated by the MEGAN model over the last 30 years, *Atmos. Chem. Phys.*, 14, 9317-
803 9341, 10.5194/acp-14-9317-2014, 2014.
- 804 Singh, H., Chen, Y., Tabazadeh, A., Fukui, Y., Bey, I., Yantosca, R., Jacob, D., Arnold,
805 F., Wohlfrom, K., Atlas, E., Flocke, F., Blake, D., Blake, N., Heikes, B., Snow, J., Talbot,
806 R., Gregory, G., Sachse, G., Vay, S., and Kondo, Y.: Distribution and fate of selected
807 oxygenated organic species in the troposphere and lower stratosphere over the Atlantic,



- 808 Journal of Geophysical Research-Atmospheres, 105, 3795-3805, 10.1029/1999jd900779,
809 2000.
- 810 Slusher, D. L., Pitteri, S. J., Haman, B. J., Tanner, D. J., and Huey, L. G.: A chemical
811 ionization technique for measurement of pernitric acid in the upper troposphere and the
812 polar boundary layer, *Geophys. Res. Lett.*, 28, 3875-3878, 10.1029/2001gl013443, 2001.
- 813 Slusher, D. L., Huey, L. G., Tanner, D. J., Chen, G., Davis, D. D., Buhr, M., Nowak, J. B.,
814 Eisele, F. L., Kosciuch, E., Mauldin, R. L., Lefer, B. L., Shetter, R. E., and Dibb, J. E.:
815 Measurements of pernitric acid at the South Pole during ISCAT 2000, *Geophys. Res. Lett.*,
816 29, 10.1029/2002gl015703, 2002.
- 817 Sorooshian, A., Ng, N. L., Chan, A. W. H., Feingold, G., Flagan, R. C., and Seinfeld, J.
818 H.: Particulate organic acids and overall water-soluble aerosol composition measurements
819 from the 2006 Gulf of Mexico Atmospheric Composition and Climate Study (GoMACCS),
820 *Journal of Geophysical Research-Atmospheres*, 112, 16, 10.1029/2007jd008537, 2007.
- 821 Sorooshian, A., Murphy, S. M., Hersey, S., Bahreini, R., Jonsson, H., Flagan, R. C., and
822 Seinfeld, J. H.: Constraining the contribution of organic acids and AMS m/z 44 to the
823 organic aerosol budget: On the importance of meteorology, aerosol hygroscopicity, and
824 region, *Geophys. Res. Lett.*, 37, 5, 10.1029/2010gl044951, 2010.
- 825 Souza, S. R., and Carvalho, L. R. F.: Seasonality influence in the distribution of formic and
826 acetic acids in the urban atmosphere of Sao Paulo City, Brazil, *Journal of the Brazilian
827 Chemical Society*, 12, 755-762, 2001.
- 828 Spaulding, R. S., Talbot, R. W., and Charles, M. J.: Optimization of a mist chamber (cofer
829 scrubber) for sampling water-soluble organics in air, *Environmental Science &
830 Technology*, 36, 1798-1808, 10.1021/es011189x, 2002.
- 831 Talbot, R. W., Beecher, K. M., Harriss, R. C., and Cofer, W. R.: Atmospheric
832 Geochemistry of Formic and Acetic Acids at a Mid-latitude Temperate Site, *Journal of
833 Geophysical Research-Atmospheres*, 93, 1638-1652, 10.1029/JD093iD02p01638, 1988.



- 834 Talbot, R. W., Mosher, B. W., Heikes, B. G., Jacob, D. J., Munger, J. W., Daube, B. C.,
835 Keene, W. C., Maben, J. R., and Artz, R. S.: Carboxylic Acids in the Rural Continental
836 Atmosphere over the Eastern United States during the Shenandoah Cloud and
837 Photochemistry Experiment, *Journal of Geophysical Research-Atmospheres*, 100, 9335-
838 9343, 10.1029/95jd00507, 1995.
- 839 Talbot, R. W., Dibb, J. E., Scheuer, E. M., Blake, D. R., Blake, N. J., Gregory, G. L.,
840 Sachse, G. W., Bradshaw, J. D., Sandholm, S. T., and Singh, H. B.: Influence of biomass
841 combustion emissions on the distribution of acidic trace gases over the southern Pacific
842 basin during austral springtime, *Journal of Geophysical Research-Atmospheres*, 104, 5623-
843 5634, 10.1029/98jd00879, 1999.
- 844 Veres, P., Roberts, J. M., Warneke, C., Welsh-Bon, D., Zahniser, M., Herndon, S., Fall, R.,
845 and de Gouw, J.: Development of negative-ion proton-transfer chemical-ionization mass
846 spectrometry (NI-PT-CIMS) for the measurement of gas-phase organic acids in the
847 atmosphere, *Int. J. Mass Spectrom.*, 274, 48-55, 10.1016/j.ijms.2008.04.032, 2008.
- 848 Veres, P., Roberts, J. M., Burling, I. R., Warneke, C., de Gouw, J., and Yokelson, R. J.:
849 Measurements of gas-phase inorganic and organic acids from biomass fires by negative-
850 ion proton-transfer chemical-ionization mass spectrometry, *Journal of Geophysical*
851 *Research-Atmospheres*, 115, 10.1029/2010jd014033, 2010.
- 852 Veres, P. R., Roberts, J. M., Cochran, A. K., Gilman, J. B., Kuster, W. C., Holloway, J. S.,
853 Graus, M., Flynn, J., Lefer, B., Warneke, C., and de Gouw, J.: Evidence of rapid production
854 of organic acids in an urban air mass, *Geophys. Res. Lett.*, 38, 10.1029/2011gl048420,
855 2011.
- 856 Vlasenko, A., George, I. J., and Abbatt, J. P. D.: Formation of volatile organic compounds
857 in the heterogeneous oxidation of condensed-phase organic films by gas-phase OH, *J. Phys.*
858 *Chem. A*, 112, 1552-1560, 10.1021/jp0772979, 2008.
- 859 Walser, M. L., Park, J., Gomez, A. L., Russell, A. R., and Nizkorodov, S. A.:
860 Photochemical aging of secondary organic aerosol particles generated from the oxidation
861 of d-limonene, *J. Phys. Chem. A*, 111, 1907-1913, 10.1021/jp066293l, 2007.



862 Xu, L., Guo, H. Y., Weber, R. J., and Ng, N. L.: Chemical Characterization of Water-
863 Soluble Organic Aerosol in Contrasting Rural and Urban Environments in the Southeastern
864 United States, *Environmental Science & Technology*, 51, 78-88, [10.1021/acs.est.6b05002](https://doi.org/10.1021/acs.est.6b05002),
865 2017.

866 Yatavelli, R. L. N., Mohr, C., Stark, H., Day, D. A., Thompson, S. L., Lopez-Hilfiker, F.
867 D., Campuzano-Jost, P., Palm, B. B., Vogel, A. L., Hoffmann, T., Heikkinen, L., Aijala,
868 M., Ng, N. L., Kimmel, J. R., Canagaratna, M. R., Ehn, M., Junninen, H., Cubison, M. J.,
869 Petaja, T., Kulmala, M., Jayne, J. T., Worsnop, D. R., and Jimenez, J. L.: Estimating the
870 contribution of organic acids to northern hemispheric continental organic aerosol,
871 *Geophys. Res. Lett.*, 42, 6084-6090, [10.1002/2015gl064650](https://doi.org/10.1002/2015gl064650), 2015.

872 Zhang, R. Y., Suh, I., Zhao, J., Zhang, D., Fortner, E. C., Tie, X. X., Molina, L. T., and
873 Molina, M. J.: Atmospheric new particle formation enhanced by organic acids, *Science*,
874 304, 1487-1490, [10.1126/science.1095139](https://doi.org/10.1126/science.1095139), 2004.

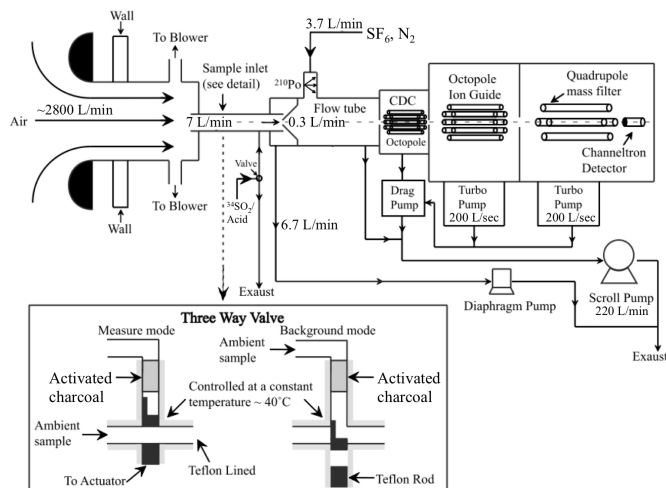
875

876

877

878

879



880

881 **Figure 1:** The CIMS instrument and inlet configuration used in the field study. The
882 automated three-way sampling valve is shown in the inset. The figure was adapted from
883 Liao et al. (2011).

884

885

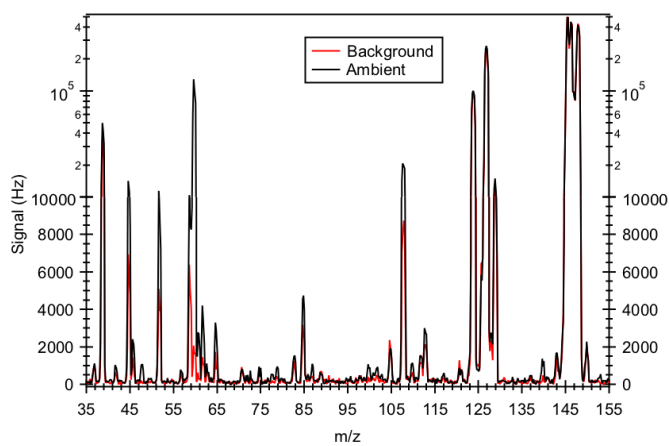
886

887

888

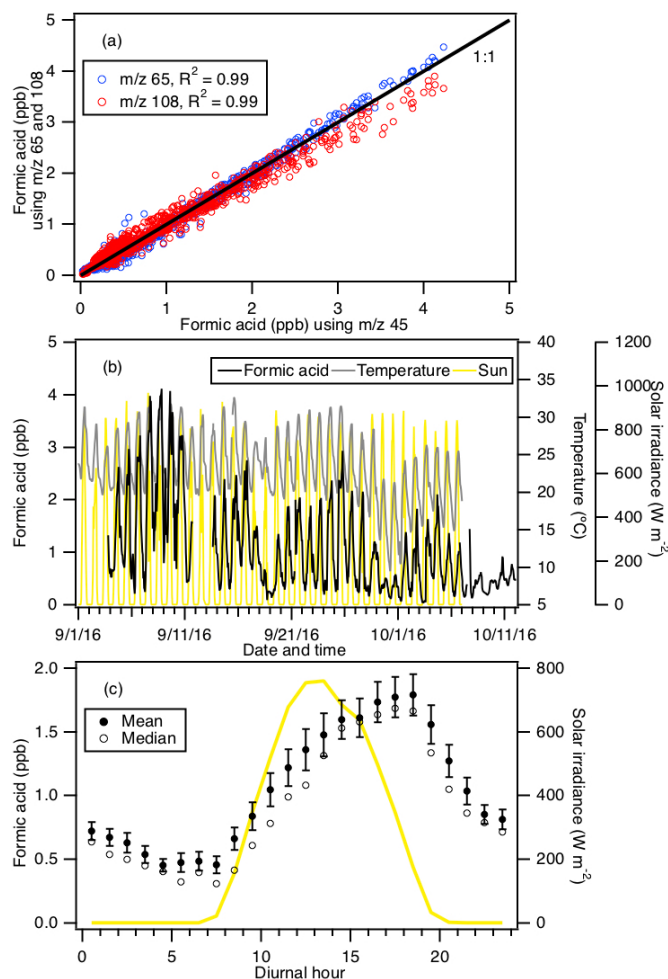
889

890



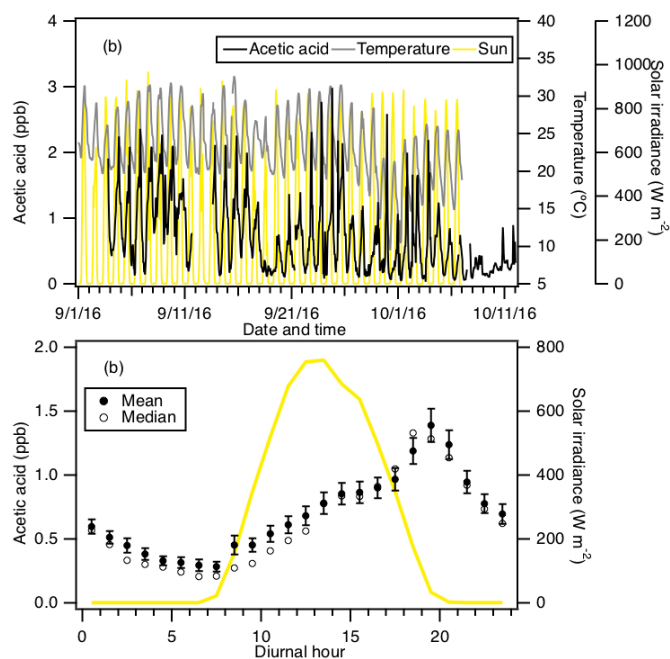
891

892 **Figure 2:** Mass spectrum of ambient air and background measured in Yorkville, Georgia
893 on 8 Sept 2016 using SF₆⁻.



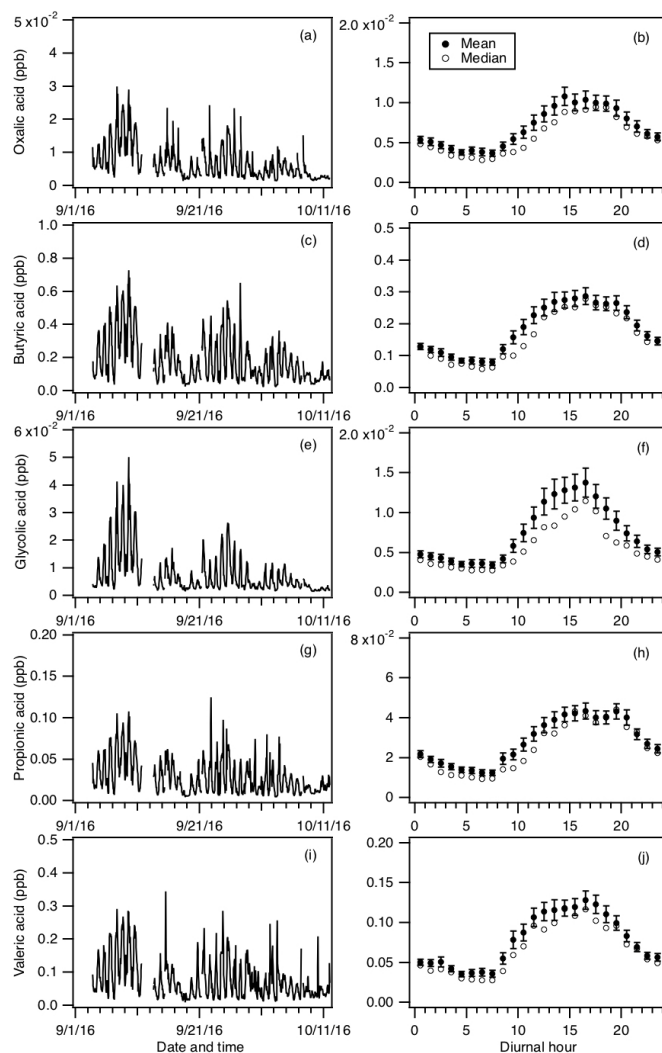
894

895 **Figure 3:** (a) Scatter plot comparison of ambient formic acid concentrations determined
896 using mass peaks m/z 45, 65 and 108. The three datasets correlated well with one another
897 ($R^2 = 0.99$). Linear regression of the data gave slopes of 1 (for m/z 65) and 0.95 (for m/z
898 108), indicating that all three mass peaks can be used to determine the formic acid
899 concentration. (b) Time series of formic acid concentration, temperature and solar
900 irradiance. All the data are displayed as 1-hour averages. (c) Diurnal profiles of formic acid
901 concentration (symbols) and solar irradiance (yellow line). All the concentrations represent
902 averages in 1-hour intervals and the standard errors are plotted as error bars.



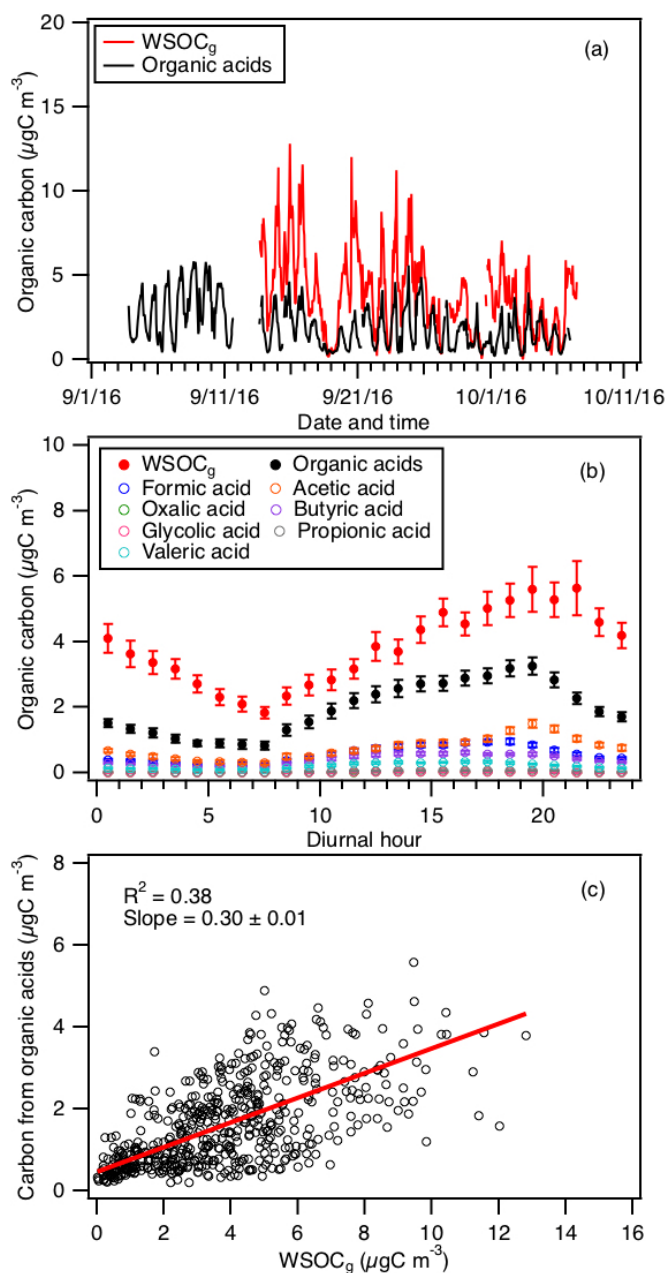
903

904 **Figure 4:** (a) Time series of acetic acid concentration, temperature and solar irradiance.
905 All the data are displayed as 1-hour averages. (b) Diurnal profiles of acetic acid (symbols)
906 and solar irradiance (yellow line). All the concentrations represent averages in 1-hour
907 intervals and the standard errors are plotted as error bars.



908

909 **Figure 5:** Time series of concentrations of (a) oxalic, (c) butyric, (e) glycolic, (g) propionic,
910 and (i) valeric acids measured during the field study. All the data are displayed as 1-hour
911 averages. Their corresponding diurnal profiles are shown in (b), (d), (f), (h) and (j),
912 respectively. The diurnal profile concentrations represent averages in 1-hour intervals and
913 the standard errors are plotted as error bars.

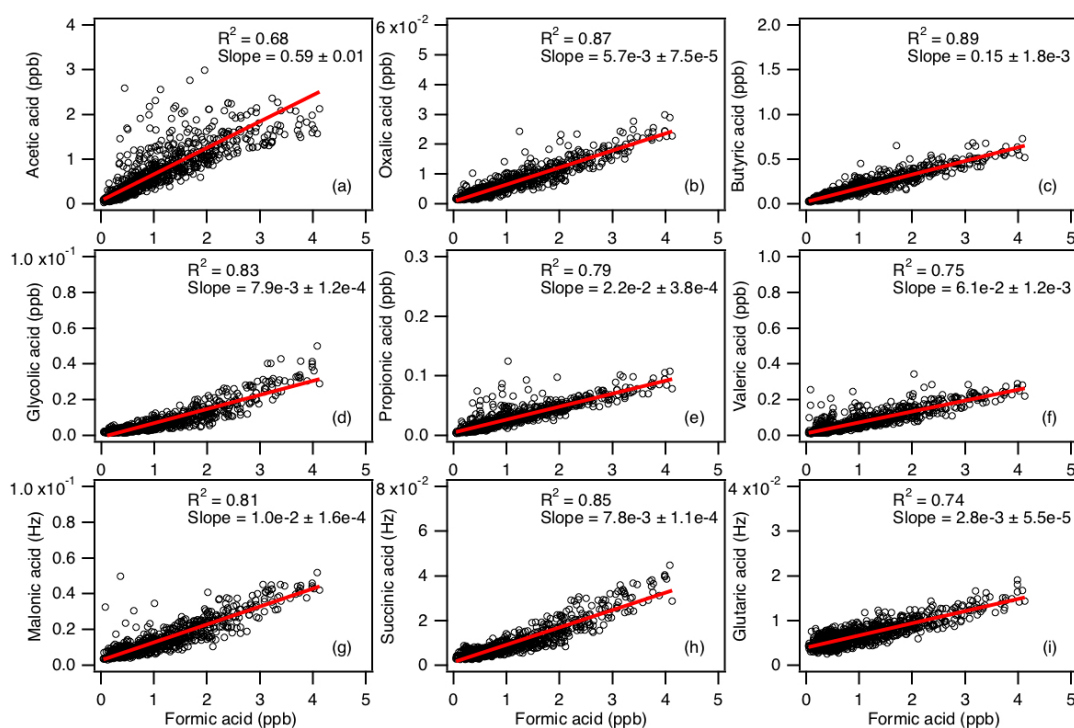


914

915 **Figure 6:** (a) Time series of WSOC_g and the total organic carbon contributed by the
 916 measured organic acids (i.e., formic, acetic, oxalic, butyric, glycolic, propionic and valeric
 917 acids). All the data are displayed as 1-hour averages. (b) Diurnal profiles of WSOC_g and
 918 the total organic carbon contributed by the measured organic acids. Also shown are the

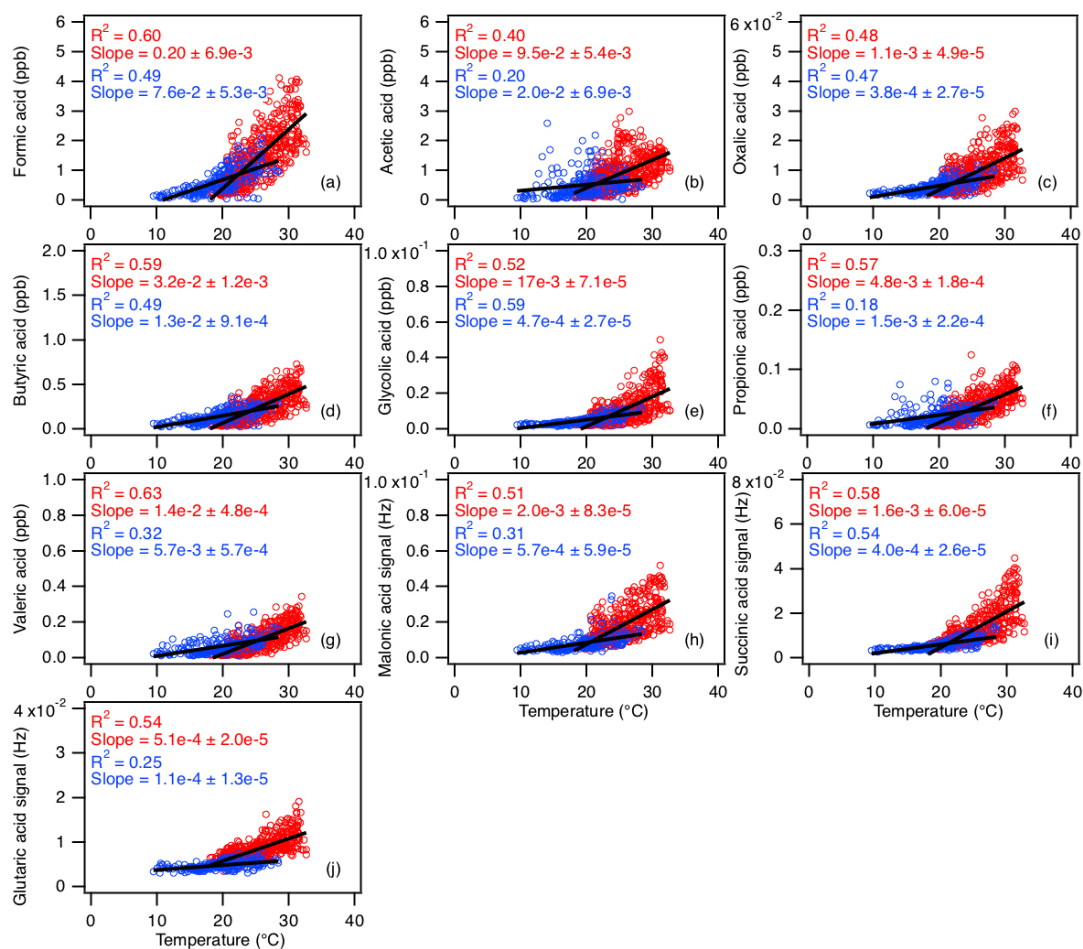


919 diurnal profiles of the organic carbon contributed by the individual measured organic acids.
920 All the concentrations represent the mean hourly averages and the standard errors are
921 plotted as error bars. (c) Scatter plot of total organic carbon contributed by the measured
922 organic acids with WSOC_g.



923

924 **Figure 7:** Scatter plots of concentrations (or signals) of (a) acetic, (b) oxalic, (c) butyric,
925 (d) glycolic, (e) propionic, (f) valeric, (g) malonic, (h) succinic, and (i) glutaric acids with
926 formic acid concentration. All the data are displayed as 1-hour averages. The data for
927 malonic, succinic and glutaric acids are presented as Hz normalized by the instrument's
928 sensitivity to $F_2^{34}SO_2$ since these organic acids were not calibrated. Red lines shown are
929 linear fits to the data.



930

931 **Figure 8:** Scatter plots of concentrations (or signals) of (a) formic, (b) acetic, (c) oxalic,
 932 (d) butyric, (e) glycolic, (f) propionic, (g) valeric, (h) malonic, (i) succinic, and (j) glutaric
 933 acids with ambient temperature. The red symbols are data collected from 3 to 27 Sept,
 934 while the blue symbols are data collected from 28 Sept onwards. All the data are displayed
 935 as 1-hour averages. The data for malonic, succinic and glutaric acids are presented as Hz
 936 normalized by the instrument's sensitivity to $F_2^{34}SO_2$ since these organic acids were not
 937 calibrated. Black lines shown are linear fits to the datasets.

938

939



940 **Table 1:** Summary of organic acids of interest, their detection limits and sensitivities of
 941 their X^- and $X^- \cdot HF$ ions relative to the $F_2^{34}SO_2^-$ ion^a

Organic Acid	Detection limit (ppb) ^b	Sensitivity relative to the $F_2^{34}SO_2^-$ ion ^c	
		X^-	$X^- \cdot HF$
Formic acid	0.03	0.44	0.10
Acetic acid	0.06	0.50	0.10
Oxalic acid	1×10^{-3}	2.18	0.33
Butyric acid	0.03	0.14	0.04
Glycolic acid	2×10^{-3}	1.89	0.56
Propionic acid	6×10^{-3}	0.70	0.43
Valeric acid	0.01	0.26	0.12

942 ^aOnly organic acids with calibration measurements are shown.

943 ^bDetection limits are approximated from 3 times the standard deviation values (3σ) of the
 944 ion signals measured during background mode. Shown here are the average detection limits
 945 of the organic acids for 2.5 min integration periods which corresponds to the length of a
 946 background measurement at a 0.04 s duty cycle for each mass.

947 ^cStudy-averaged sensitivity of the $F_2^{34}SO_2^-$ ion = 2928 ± 669 Hz ppb⁻¹